Cell, Vol. 119, 529–542, November 12, 2004, Copyright ©2004 by Cell Press

Ferritin Heavy Chain Upregulation by NF-κB Inhibits TNFα-Induced Apoptosis by Suppressing Reactive Oxygen Species

Can G. Pham,[1,2] Concetta Bubici,[1] Francesca Zazzeroni,[1,6] Salvatore Papa,[1,6] Joy Jones,[1] Kellean Alvarez,[1] Shanthi Jayawardena,[1] Enrico De Smaele,[1] Rong Cong,[1] Carole Beaumont,[3] Frank M. Torti,[4] Suzy V. Torti,[5] and Guido Franzoso[1,*]

[1]The Ben May Institute for Cancer Research and
[2]The Department of Pathology
The University of Chicago
924 East 57th Street
Chicago, Illinois 60637
[3]INSERM U409
Service d'Hematologie et d'Immunologie Biologiques
CHU Bichat
Paris
France
[4]Department of Cancer Biology and
[5]Department of Biochemistry
Wake Forest University School of Medicine
Winston-Salem, North Carolina 27157

Summary

During inflammation, NF-κB transcription factors antagonize apoptosis induced by tumor necrosis factor (TNF)α. This antiapoptotic activity of NF-κB involves suppressing the accumulation of reactive oxygen species (ROS) and controlling the activation of the c-Jun N-terminal kinase (JNK) cascade. However, the mechanism(s) by which NF-κB inhibits ROS accumulation is unclear. We identify ferritin heavy chain (FHC)—the primary iron storage factor—as an essential mediator of the antioxidant and protective activities of NF-κB. FHC is induced downstream of NF-κB and is required to prevent sustained JNK activation and, thereby, apoptosis triggered by TNFα. FHC-mediated inhibition of JNK signaling depends on suppressing ROS accumulation and is achieved through iron sequestration. These findings establish a basis for the NF-κB-mediated control of ROS induction and identify a mechanism by which NF-κB suppresses proapoptotic JNK signaling. Our results suggest modulation of FHC or, more broadly, of iron metabolism as a potential approach for anti-inflammatory therapy.

Introduction

In addition to marshalling immune and inflammatory responses, NF-κB transcription factors control apoptosis or programmed cell death (PCD) (Kucharczak et al., 2003). Activation of NF-κB antagonizes PCD induced by tumor necrosis factor (TNF)α. The antiapoptotic activity of NF-κB is also crucial for B lymphopoiesis, oncogenesis, and cancer chemoresistance (Orlowski and Baldwin, 2002; Gerondakis and Strasser, 2003; Kucharczak et al., 2003). With regard to TNFα, the inhibition of PCD by NF-κB depends on suppression of the c-Jun N-terminal kinase (JNK) cascade (De Smaele et al., 2001; Javelaud and Besancon, 2001; Tang et al., 2001).

JNK1/2/3 are downstream components of a major mitogen-activated protein kinase (MAPK) cascade (Davis, 2000; Chang and Karin, 2001). Acute JNK induction by TNF receptors (TNF-Rs) likely involves MAPK kinase kinases (MAPKKKs) of the MAPK/ERK kinase (MEK) and mixed lineage kinase (MLK) groups (Davis, 2000). Conversely, the sustained phase of JNK activation downstream of TNF-Rs, and thereby apoptosis, depends on ASK1/MEKK5 (Matsuzawa et al., 2002)—a TRAF2 binding MAPKKK. Activation of ASK1 in turn requires reactive oxygen species (ROS), which inactivate the ASK1 inhibitor, thioredoxin (Trx) (Matsuzawa et al., 2002). Indeed, ROS appear to be key mediators of TNFα-induced apoptosis (Garg and Aggarwal, 2002; Matsuzawa et al., 2002; Sakon et al., 2003). ROS are also critically involved in PCD triggered by other stimuli, including ceramide, radiation, and chemotherapeutic agents. Accordingly, treatment with oxidants is sufficient to induce apoptosis (Curtin et al., 2002; Fleury et al., 2002). Cytotoxicity caused by ROS is mediated in part by the JNK pathway (Matsuzawa et al., 2002). Activation of this pathway by TNFα promotes death by inducing cleavage of the Bcl-2 family BH3-only protein, Bid, into jBid, which targets mitochondria to trigger release of Smac/Diablo into cytosol, leading to activation of caspase-8 (Deng et al., 2003). ROS can also mediate caspase-independent, necrosis-like cell death (Leist and Jaattela, 2001).

In eukaryotes, the main source of oxygen radicals is mitochondria (Curtin et al., 2002; Fleury et al., 2002). Here, molecular oxygen is converted into superoxide anion ($O_2^{\cdot -}$), a moderately reactive species capable of generating hydrogen peroxide (H_2O_2), which in turn can produce highly reactive hydroxyl radicals (·OH) via metal-dependent breakdown (Curtin et al., 2002). Cells possess effective mechanisms to control ROS. Among these is the synthesis of enzymes such as superoxide dismutases (SODs), catalase, and glutathione peroxidases (Gpxs), which convert ROS into less-active species (Curtin et al., 2002; Fleury et al., 2002). Another powerful strategy that cells have adopted to overcome ROS is to limit the cellular availability of transition metals, most notably iron. Indeed, this metal catalyzes the generation of $O_2^{\cdot -}$ in mitochondria and participates in Fenton and Haber-Weiss reactions leading to formation of ·OH (Curtin et al., 2002; Torti and Torti, 2002). This control of iron levels is achieved in part through metal sequestration mediated by synthesis of ferritin—the major iron storage mechanism (Arosio and Levi, 2002; Torti and Torti, 2002).

Interestingly, ROS accumulation in response to TNFα is regulated in an NF-κB-dependent manner (Sakon et al., 2003). However, the mechanism(s) by which NF-κB controls ROS accumulation is not clear. To understand the basis for the protective activity of NF-κB and identify

*Correspondence: gfranzos@midway.uchicago.edu
[6]These authors contributed equally to this work.

Table 1. Enrichment in ROS Regulators after Library Selection in *relA*$^{-/-}$ Cells

Gene Name	Msa No.	SI_E	SI_O	$SLR_{E/O}$	Refs.
Apoptosis					
FADD	Msa.2049.0_at	210384.1	467.6	8.5	1 and 2
PPX	Msa.17599.0_at	485121.4	3710.5	7.3	3–5
RelA	Msa.1018.0_at	266918.6	3017.5	5.9	6 and 7
UFO/AXL receptor	Msa.2518.0_at	222342	8597.2	4.9	8–10
ASM-1	Msa.2164.0_at	8781.1	443.6	4.2	11 and 12
Cathepsin L	Msa.547.0_at	194898.7	12898.9	3.8	13–15
Cardiotrophin-1	Msa.1448.0_at	3476	285.9	3.7	16 and 17
Thymosin β4	Msa.1236.0_i_at	3787.5	273.8	3.7	18 and 19
VEGF	Msa.1279.0_at	9045.7	994	3.3	20 and 21
c-Jun	Msa.535.0_at	3485.1	281.4	3.1	22 and 23
PDGF receptor	Msa.2594.0_at	3858.9	499	3	24 and 25
MDR-1	Msa.1675.0_at	16380.8	2773.1	2.7	26 and 27
α1-AGP	Msa.413.0_at	7281.7	1542.5	2.6	28
Krox-20	Msa.881.0_at	2324.1	425.9	2.6	29 and 30
GAPDH	Msa.677.0_at	79463.6	17006.3	2.5	31 and 32
M-Twist	Msa.1265.0_at	3353.2	581.5	2.5	33 and 34
HSP105	Msa.1937.0_at	6685.7	2656	2	35 and 36
c-MYC	Msa.2088.0_at	2162.7	545.3	2	37 and 38
ROS and Iron Metabolism					
Glutathione peroxidase-4	Msa.14493.0_at	10676.9	251.5	4.8	39
Uroporphyrinogen decarboxylase	Msa.1781.0_at	6052.3	483.7	4	40 and 41
Heme oxygenase-1	Msa.1044.0_at	22789.5	3875.3	2.6	42 and 43
Ferritin heavy chain	Msa.643.0_at	376017.5	67902.8	2.2	44 and 45
Cytochrome P-450IIIA	Msa.2228.0_i_at	1342	434.9	1.8	46
(Catalase)	Msa.505.0_at	1105	528.2	0.4	47
(Mn-superoxide dismutase)	Msa.1633.0_at	1032.5	2618	−1.3	48
(Ferritin light chain)	Msa.644.0_l_at	1823.7	21797.3	−3.2	44 and 45

Partial list of cDNAs enriched upon selection. Genes are grouped by function and ranked according to their SLR values. Msa No., Affymetrix probe identification number; SI_E and SI_O, signal intensity values with probes prepared from enriched and original libraries, respectively; $SLR_{E/O}$, SLR of SI_E versus SI_O. Selected ROS scavengers that scored poorly (i.e., SLR <1) in the screen are in parentheses. Relevant references (Refs.) are listed in the Supplemental Data.

genes that mediate the suppression of ROS by NF-κB, we performed a systematic screen of libraries enriched in antiapoptotic cDNAs using microarrays. Using this approach, we identified ferritin heavy chain (FHC) as a pivotal mediator of the NF-κB protective activity against TNFα-induced toxicity. FHC is one of two subunits of ferritin, a heteropolymer that also consists of light chains (FLC) (Arosio and Levi, 2002; Torti and Torti, 2002). Unlike FLC, FHC exhibits ferroxidase activity—required for iron sequestration (Arosio and Levi, 2002) —and is under tight regulation by cytokines and oncogenes (Torti and Torti, 2002). Here, we show that FHC, rapidly induced by TNFα in an NF-κB-dependent manner, is essential for suppressing TNFα-induced killing and blocks PCD in NF-κB/RelA null cells. The antiapoptotic activity of FHC functions to inhibit induction of ROS and, thereby, activation of JNK by TNFα. Together, these findings establish a mechanism for NF-κB-mediated control of ROS accumulation and apoptosis induced by TNFα. The data also unravel a mechanism by which NF-κB inhibits the JNK cascade.

Results

Systematic Analysis of Genes Capable of Blocking PCD in *relA*$^{-/-}$ Cells

To understand the mechanisms by which TNFα induces apoptosis and to define the basis for the protective activity of NF-κB, we have employed the "death trap" screen in *relA*$^{-/-}$ cells (De Smaele et al., 2001; Vito et al., 1996). Expression libraries were transfected into these cells by the use of the DEAE method, and apoptosis was induced with TNFα. Plasmids were then recovered from surviving cells, and the resulting pooled cDNAs were amplified in *E. coli* and used for subsequent rounds of selection in *relA*$^{-/-}$ cells, as described previously (De Smaele et al., 2001). This system previously yielded libraries highly enriched in antiapoptotic cDNAs, including those encoding RelA, the JNK pathway inhibitor Gadd45β, the catalytically inactive relative of caspase-8 c-FLIP$_L$, and dominant-negative (DN) variants of the caspase-8 activator FADD (De Smaele et al., 2001). Finally, enrichment of antiapoptotic cDNAs was confirmed by PCR, using libraries as templates and *relA*- or β-*actin*-specific primers (data not shown).

To identify cDNAs that were enriched during selection, we utilized gene array technology. Original and selected libraries were transcribed in vitro to generate cRNA probes. These were then used to interrogate pairs of Mu6500 microchips (Affymetrix)—which contain ~6,500 oligonucleotide sets derived mainly from known genes. Putative antiapoptotic cDNAs were defined as those that increased in frequency during selection and so yielded stronger hybridization signals with probes prepared from the enriched libraries than with probes prepared from the original library. Since this approach required

no information about gene sequence and/or function, it offered an unbiased method for isolating genes capable of blocking apoptosis in NF-κB null cells.

This gene chip system also allowed clustering of isolated genes based upon their putative function, thereby unmasking cellular defects caused by loss of NF-κB. Moreover, it enabled ranking of these genes according to their signal log ratio (SLR) score, which correlates with the degree of enrichment during selection and so provides a semiquantitative indication of antiapoptotic efficacy. Of the genes represented in the Mu6500 chip, 90 exhibited SLR values higher than 1 (data not shown). These genes (or fragments of these genes) were therefore those most highly enriched by selection, as determined by the use of this chip. Validating our approach, RelA and DN-FADD ranked eighth and second according to this value (5.9 and 8.5, respectively; Table 1).

The Suppression of ROS Is a Protective Mechanism Mediated by NF-κB

One group of genes enriched by selection with TNFα encoded factors previously associated with ROS metabolism and/or iron homeostasis (Table 1; Curtin et al., 2002; Fleury et al., 2002). This finding suggests that defects in these metabolic systems contribute to the susceptibility of RelA null cells to TNFα-induced toxicity. Therefore, we tested whether ablation of RelA affected changes in redox status during TNFα stimulation. In *relA*$^{-/-}$ cells transduced with empty MSCV vectors, ROS progressively accumulated, beginning 2 hr after TNFα treatment. In contrast, in cells transduced with MSCV-RelA, TNFα-induced ROS accumulation was markedly suppressed (Figure 1A). The antioxidant activity of RelA was specific for TNFα, as RelA expression did not affect ROS induction by antimycin A (Figure 1B)—a poison of the mitochondrial respiratory chain (Chandel et al., 2001). Hence, the control of ROS induction by TNF-R triggering is a physiologic function of NF-κB.

Importantly, control of ROS is crucial for NF-κB to suppress TNFα-induced PCD. As shown in Figure 1C, pretreatment with the antioxidant, NAC, almost completely rescued *relA*$^{-/-}$ fibroblasts from TNFα-induced death in a dose-dependent manner. Similar findings were obtained with PDTC—another blocker of ROS (Figure 1D). The protective effects of antioxidant agents extended to other NF-κB-deficient cell types. For example, 3DO T cell clones expressing IκBαM—an inhibitor of NF-κB—were highly sensitive to TNFα-induced killing, whereas control 3DO clones (Neo) were not (Figure 1F; see also De Smaele et al. [2001]). The susceptibility of IκBαM-expressing cells to cytotoxicity by TNFα was blocked by antioxidant treatment, and protection afforded by this treatment was virtually complete even at late times (16 hr; compare survival of Neo and PDTC-treated, IκBαM clones; see also Supplemental Figure S1 at http://www.cell.com/cgi/content/full/119/4/529/DC1/). Similar protective effects of antioxidants have been reported by others (Sakon et al., 2003). We concluded that NF-κB blocks TNFα-induced PCD, at least in part, by upregulating genes that suppress production and/or promote disposal of ROS.

In both *relA*$^{-/-}$ fibroblasts and 3DO-IκBαM cells, TNFα cytotoxicity was abrogated by the pancaspase inhibitor, z-VAD$_{fmk}$ (Figures 1E and 1F, respectively; see also Supplemental Figure S1 on the *Cell* web site), indicating that, in these cells, TNFα induces death mainly through an apoptotic mechanism. Indeed, TNF-R triggering induced DNA fragmentation and caspase activation (Figures 1C–1F and Figure 4A; also data not shown)—two hallmarks of apoptosis (Danial and Korsmeyer, 2004). Thus, although ROS can promote caspase-independent, necrosis-like death in some systems (Leist and Jaattela, 2001), these species appear to induce death by apoptosis in NF-κB-deficient cells.

FHC Is Transcriptionally Regulated by NF-κB

Since a deficiency in NF-κB activity leads to apoptosis via ROS generation, we examined whether any of the ROS blockers isolated from our "death trap" screen (see Table 1) were subject to regulation by NF-κB. As shown in Figures 2A and 2B, *fhc* was induced rapidly by TNFα in control 3DO cells (Neo and parental, respectively) but not in 3DO cells expressing IκBαM. This induction mirrored the expression of *p50/p105* (data not shown), a known target of NF-κB (Ghosh et al., 1998). *fhc* was also upregulated by TNFα in wild-type mouse embryonic fibroblasts (MEFs), and this upregulation was impaired in RelA null cells (Figure 2C).

Conversely, expression of other ROS modulators, including *gpx-1* and *-4*, *cytochrome P-450III*, and *cytochrome oxidase I*, as well as of *thioredoxin*, was unaffected by either TNFα or NF-κB (Figure 2A and data not shown). *Heme oxygenase-1* (*ho-1*) was upregulated by TNFα but only at late times (Figure 2B and data not shown). Moreover, induction of *ho-1* by PMA plus ionomycin (P/I) was independent of NF-κB (Figure 2D). Mn^{2+} *superoxide dismutase* (*Mn-sod*)—a ROS scavenger that scored poorly in our screen (Table 1)—was upregulated by TNFα in wild-type but not in *relA*$^{-/-}$ MEFs (Figure 2C). However, in 3DO cells, *Mn-sod* was not induced by either TNFα or P/I (Figures 2A, 2B, and 2D), indicating that its expression is controlled by cell type-specific mechanisms. Altogether, the data indicate that *fhc* is a TNFα-inducible gene and a downstream target of NF-κB. Conversely, other ROS blockers isolated from our screen do not appear relevant to the antiapoptotic function of NF-κB, and Mn-SOD may be relevant to this function only in certain tissues.

Because FHC is also subject to posttranscriptional regulation (Torti and Torti, 2002), we sought to confirm the physiologic relevance of FHC induction by NF-κB by performing Western blots. As shown in Figure 2E, TNFα failed to upregulate FHC in *relA*$^{-/-}$ fibroblasts transduced with empty MIGR1 vectors. This upregulation was promptly restored upon complementation with MIGR1-RelA. To further link FHC induction by TNFα to NF-κB, we used the HeLa-derived HtTA-RelA and HtTA-p50 lines, where NF-κB activation can be achieved by tetracycline withdrawal, independently of cellular stimulation (Zong et al., 1999). As shown in Figure 2F, tetracycline removal prompted upregulation of FHC in HtTA-RelA cells but not in control HtTA-1 cells or HtTA-p50 cells, which conditionally express p50—a subunit of NF-κB that lacks activation domains (Ghosh et al., 1998). The FHC pattern of expression paralleled that of IκBα—another target of NF-κB (Ghosh et al., 1998). Hence,

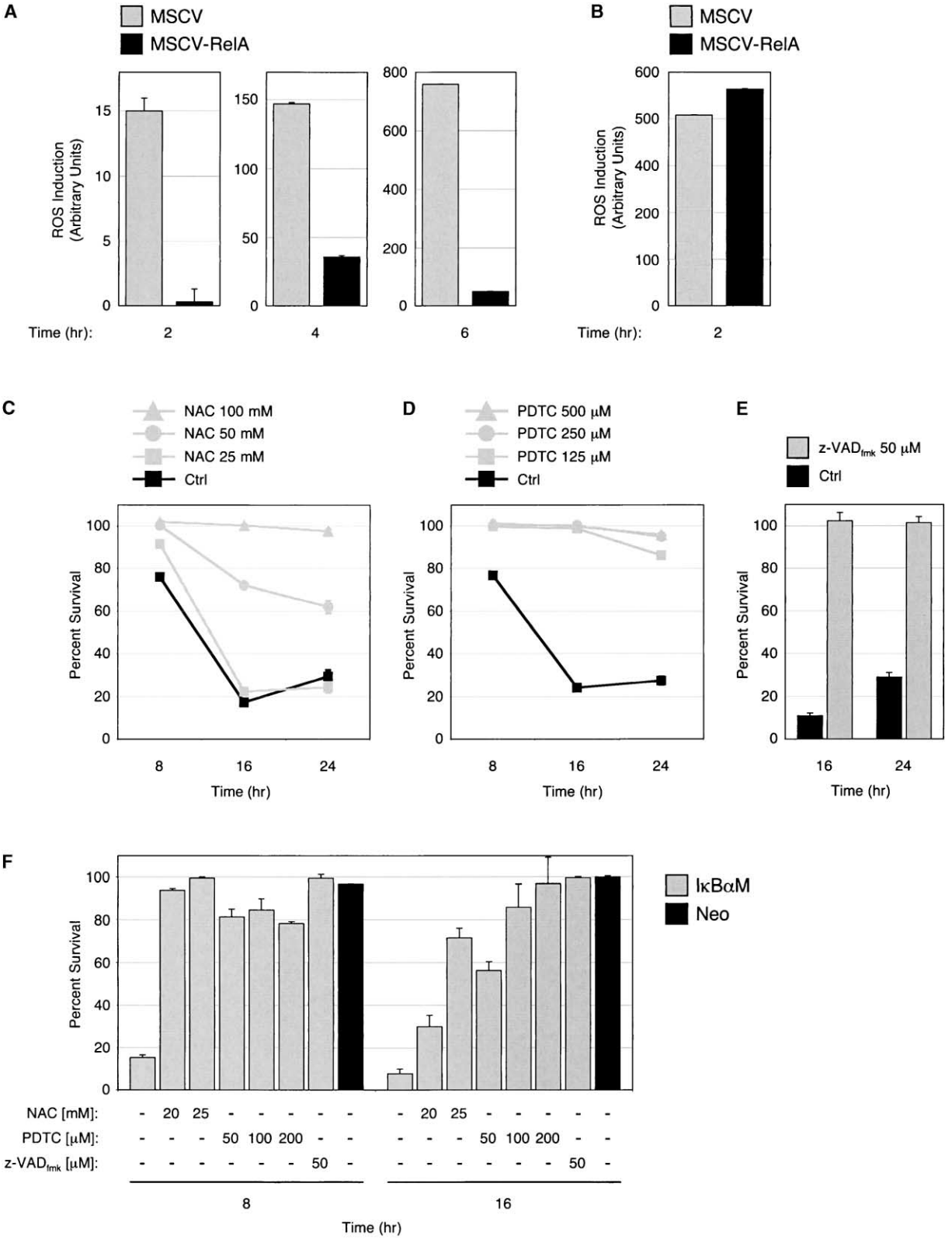

Figure 1. The Suppression of ROS Is a Protective Mechanism Mediated by NF-κB

(A) ROS induction by TNFα in MSCV- and MSCV-RelA-transduced *relA*$^{-/-}$ cells. Cells were treated with TNFα (100 U/ml) plus CHX (0.1 μg/ml), and ROS levels were measured at the indicated times by spectrofluorometric analysis. Columns represent fluorescence units after subtraction of the background values obtained with CHX-treated cultures and are the mean (± standard deviation) of three independent measurements.

activation of NF-κB/RelA is sufficient to upregulate FHC. Altogether, the findings suggest that FHC induction by TNFα involves a transcriptional mechanism controlled by NF-κB and underscore the importance of RelA in this mechanism.

FHC Is a Physiologic Blocker of TNFα-Induced Killing

To ensure that induction of FHC by NF-κB serves a protective function, we monitored the effects of ectopic expression of FHC on TNF-R-triggered PCD. Upon transduction with MIGR1-FHC retroviruses expressing FLAG-tagged FHC, *relA*$^{-/-}$ cells were markedly protected against TNFα-induced death, whereas cells infected with empty MIGR1 were not (Figure 3A; see also Supplemental Figure S2A, primary RelA null cells). As expected, with MIGR1-RelA, rescue was complete (data not shown). Resistance to apoptosis correlated with FHC levels (Figures 3B and 3C) and was nearly complete at early times (Figure 3A, 8 hr), suggesting that FHC is sufficient to temporarily suppress TNFα-induced PCD. Importantly, the FHC levels capable of affording near-complete protection in *relA*$^{-/-}$ cells (Figures 3A and 3B, relative viral dose 1) approximate those achieved in wild-type NIH-3T3 fibroblasts during stimulation with TNFα and found constitutively in certain primary tissues (e.g., the embryonic liver) and cell lines (Figure 3D and Supplemental Figure S2B, respectively; compare to MIGR1-FHC; note that, in Figure 3D, MIGR1-FHC expression is similar to that of the highest viral dose in Figure 3C). In fact, cytoprotection was dramatic even at lower FHC levels (Figures 3B and 3C; see relative viral doses 1/2 and 1/4). In contrast, overexpressed Mn-SOD afforded limited protection against PCD triggered by TNFα (Figures 3B and 3C). These results, along with those from our microchip screen (Table 1), show that FHC is a potent blocker of TNFα-induced apoptosis and a novel mediator of the protective function of NF-κB.

To further verify that physiologic levels of FHC were cytoprotective, we used RNA interference (RNAi). In NIH-3T3 fibroblasts, FHC was effectively knocked down by expression of *fhc*-specific siRNAs, as shown by Western blots (Figure 3E, bottom; see *fhc-198*). Silencing was specific, since these siRNAs did not affect expression of β-actin or Lamin-A/C (Figure 3E and data not shown). Furthermore, three different siRNA controls had no effect on FHC levels (Figure 3E; see also Supplemental Figure S3). Remarkably, FHC downregulation markedly increased susceptibility of NIH-3T3 cells to TNFα-induced killing (Figures 3E, top, and Figure 3F), despite normal activation of NF-κB (data not shown). Cytotoxicity correlated with the extent of FHC downregulation (data not shown). Confirming the specificity of the observed effects, NIH-3T3 cells expressing control siRNAs remained refractory to cytokine-induced PCD (Figures 3E and 3F).

Of note, the effect of the *fhc-198* siRNA on cell survival was comparable to that of *relA*-specific siRNAs (Supplemental Figure S3), which suggests that, in these cells, FHC is a dominant component of the antiapoptotic mechanism activated by NF-κB. Similar findings were obtained with *fhc*- and *relA*-specific siRNAs in the HeLa-derived line, HtTA-RelA (Supplemental Figures S4A and S4B), indicating that this dominance of the FHC protective activity against TNFα-induced PCD extends to other cell types and species (see Discussion). We concluded that induction of FHC by NF-κB is critically required to antagonize TNF-R-induced apoptosis and that defects in this induction likely contribute to the propensity of *relA*$^{-/-}$ cells to undergo PCD.

FHC Inhibits Apoptosis Signaling in NF-κB Null Cells

To understand how FHC confers protection from PCD induced by TNFα, we examined the effects of FHC on caspase activation. In MIGR1-transduced *relA*$^{-/-}$ fibroblasts, caspase-8 processing was detected as early as 6 hr after treatment with TNFα, with progressive proteolysis of the proenzyme and accumulation of p41/p43 cleavage intermediates thereafter (Figure 4A). This coincided with activation of the caspase-8 substrate Bid as well as of downstream procaspase-9 and -3 (Figure 4A, MIGR1; see degradation of protein proforms and appearance of cleavage products). Proteolysis was specific, since control proteins such as β-actin were not degraded in the cell extracts (Figure 4A) and coincided with a marked increase in caspase-8, -9, and -3/-7 activities (data not shown). As expected, these events were abrogated by expression of RelA (data not shown). Remarkably, TNFα-induced caspase activation was also suppressed by FLAG-FHC (Figure 4A). In MIGR1-FHC-transduced *relA*$^{-/-}$ cells, procaspases and Bid remained virtually intact throughout stimulation with TNFα, with modest accumulation of caspase-3 products seen only at late times.

FHC also inhibited mitochondrial depolarization—another key event in TNF-R-induced apoptosis (Danial and Korsmeyer, 2004). In RelA null fibroblasts, the mitochondrial transmembrane potential began to drop 6 hr after treatment with TNFα, with ~60% of the cells exhib-

(B) ROS induction by a 2 hr treatment with antimycin A (1 μg/ml). Cells and ROS measurements were as in (A). Shown are the values obtained after subtraction of background from untreated cells.
(C) PI nuclear staining assays showing survival of *relA*$^{-/-}$ cells after treatment with TNFα (100 U/ml) plus CHX (0.1 μg/ml), in the absence or presence of a 1 hr pretreatment with the indicated concentrations of NAC. Values represent the percentages of live cells (i.e., with DNA content ≥N2) relative to cultures treated with CHX alone and are the mean ± standard deviation of three independent experiments.
(D) PI nuclear staining assays showing survival of *relA*$^{-/-}$ cells treated as in (C), in the absence or presence of a 1 hr pretreatment with the indicated concentrations of PDTC. Values are the mean ± standard deviation of three independent experiments and were calculated as in (C).
(E) PI nuclear staining showing survival of *relA*$^{-/-}$ cells treated as in (C), in the absence (Ctrl.) or presence of a 1 hr pretreatment with z-VAD$_{fmk}$. Values are the mean ± standard deviation of three independent experiments and were calculated as in (C).
(F) PI nuclear staining assays showing survival of 3DO IκBαM clones after treatment with TNFα (50 U/ml) in the presence or absence of a 1 hr pretreatment with the indicated agents. Times and concentrations are shown. Neo control clones are in black. Values are the mean ± standard deviation of three independent experiments and were calculated as in (C).

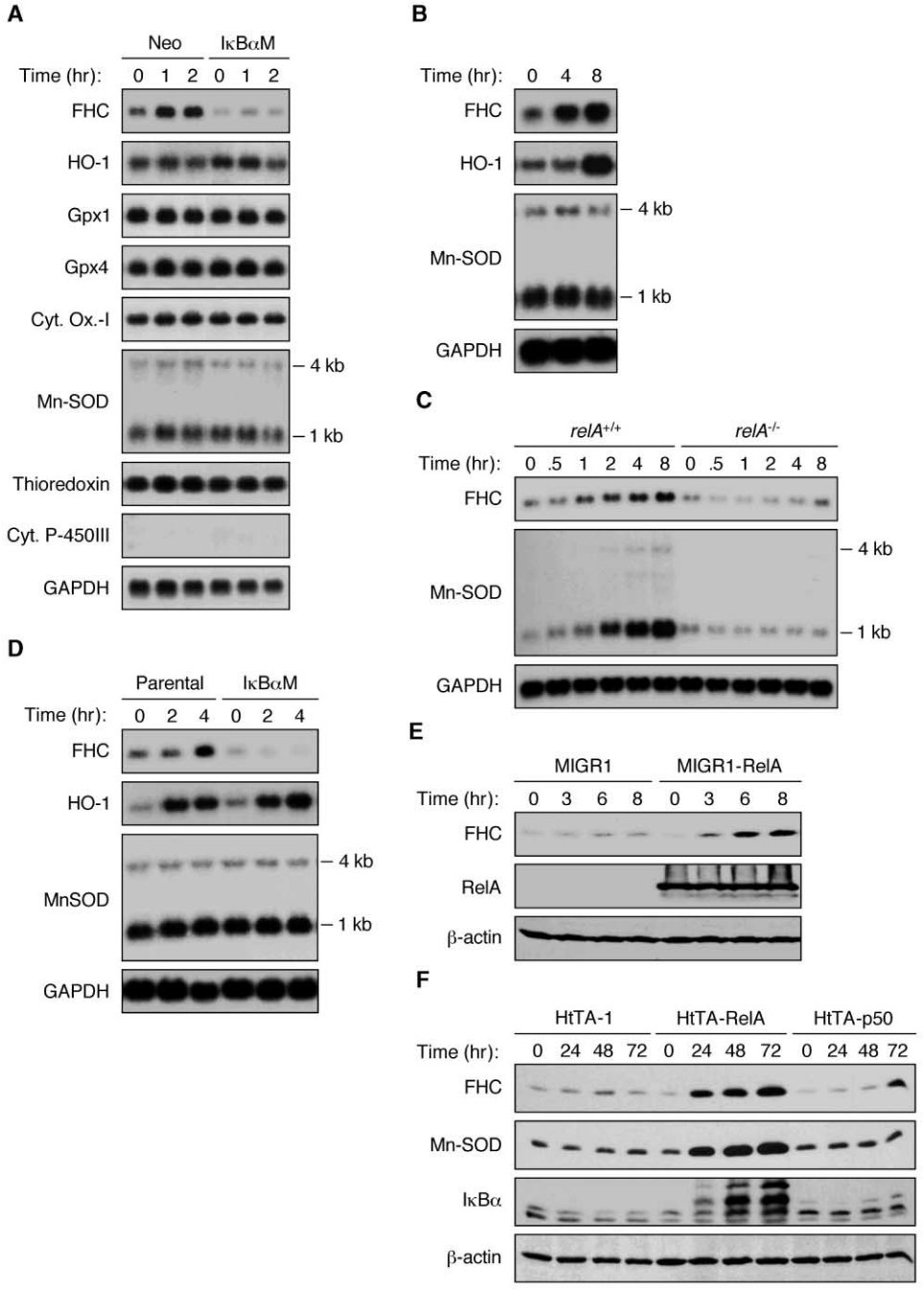

Figure 2. FHC Is a Physiological Target of NF-κB

(A) Northern blots showing expression of ROS regulators in Neo and IκBαM 3DO clones treated with TNFα (1,000 U/ml) for the times shown. HO-1, heme oxygenase-1; Gpx, glutathione peroxidase; Cyt. Ox.-I, cytochrome oxidase subunit I; Cyt. P-450III, cytochrome P-450 IIIA.

(B) Northern blots showing expression of the indicated genes in parental 3DO cells treated as in (A).

(C) Northern blots showing expression of the indicated genes in early passage (p8) MEFs derived from twin *relA*$^{+/+}$ and *relA*$^{-/-}$ embryos and treated with TNFα (1000 U/ml).

(D) Northern blots showing expression of the indicated genes in parental and IκBαM 3DO cells treated with PMA (50 ng/ml) plus ionomycin (1 μM).

(E) Western blots showing induction of FHC in MIGR1- and MIGR1-RelA-transduced *relA*$^{-/-}$ cells after cytotoxic treatment with TNFα (1000 U/ml) plus low doses of CHX (0.1 μg/ml). Exogenous RelA is shown.

(F) Western blots showing levels of the indicated proteins in the HtTA-RelA and HtTA-p50 lines and in control HtTA-1 cells following tetracycline withdrawal. Induction of p50 and RelA transgenes was verified experimentally (data not shown).

iting depolarized mitochondria by 12 hr (Figure 4B; MIGR1). As expected, this drop was abrogated by complementation with MIGR1-RelA (Supplemental Figure S5). Depolarization was almost completely inhibited also by FHC (Figure 4B; MIGR1-FHC). Thus, FHC blocks TNFα-induced caspase activation and mitochondrial depolarization in NF-κB-deficient cells, thereby recapitulating the effects of NF-κB on apoptosis pathways.

FHC Prevents ROS Induction and Apoptosis via Iron Sequestration

The observation that FHC protected NF-κB null cells from TNFα-induced PCD prompted us to investigate whether FHC mediated the inhibition of ROS by NF-κB (Figure 1A). Remarkably, FHC suppressed ROS induction in response to TNFα in RelA null cells (Figure 5A; MIGR1-FHC). To determine whether iron binding was involved in this suppression, we then tested the effects of FHC-222, a variant of FHC that lacks iron binding activity (Torti and Torti, 2002). As shown in Figure 5A, expression of this mutant failed to block ROS accumulation induced by TNFα, indicating that FHC-mediated blockade of ROS requires iron sequestration. As seen with RelA (Figures 1A and 1B), the inhibitory effects of FHC were specific for the TNFα pathway, as neither mutant nor wild-type FHC affected ROS elevation following antimycin A treatment (Figure 5A). Hence, FHC mimics the effects of NF-κB on redox changes during extracellular challenge.

Given the critical role of ROS in TNF-R apoptotic signaling, we tested whether the protective activity of FHC also depended on iron binding. As shown in Figure 5B, FHC-222 failed to inhibit TNFα-induced killing in *relA*$^{-/-}$ cells. This lack of activity was not due to protein instability or poor expression, as in these cells, FHC-222 levels were comparable to those of wild-type FHC (Figure 5B, bottom). It has been proposed by others that, in certain NF-κB-proficient systems, FHC promotes survival by mechanisms independent of its iron binding activity (Cozzi et al., 2003). The nature of these mechanisms, however, is unclear. Thus, to clarify this issue, we monitored the effects of metal removal by means other than FHC expression on cell survival. As shown in Figure 5C, pretreatment with DFO—a well-characterized iron chelator (Torti and Torti, 2002; see also Supplemental Data)—dramatically inhibited TNFα-induced PCD in RelA null cells in a dose-dependent manner. Similar protective effects of DFO have been reported by others in several additional mouse and human systems (Smirnov et al., 1999; Brouard et al., 2000; Vulcano et al., 2000). Hence, iron plays a critical role in mediating TNF-R apoptotic signaling, and this appears to be the case in many tissues. Curiously, in the HeLa-derived clones used by Cozzi et al., iron inhibited rather than promoted TNFα-induced killing (Cozzi et al., 2003), which suggests that these authors' findings with FHC are due to an atypical behavior of iron in these clones. Altogether, the data indicate that the antioxidant activity of FHC involves iron sequestration and that this sequestration is crucial for suppression of apoptosis induced by TNFα. Indeed, the FHC-mediated blockade of ROS appears to be an essential component of the NF-κB protective function.

ROS-Induced Cytotoxicity Is Mediated by the JNK Pathway

The NF-κB-mediated control of TNFα-induced PCD involves suppression of JNK signaling (De Smaele et al., 2001; Javelaud and Besancon, 2001; Tang et al., 2001). Thus, we examined whether inductions of JNK and ROS by TNFα are linked or whether they represent independent cytotoxic mechanisms. In RelA null fibroblasts, sustained JNK induction by TNFα was almost completely blocked by treatment with NAC (Figure 6A), whereas the acute phase of this induction was affected only modestly by this treatment. Similar findings were obtained with BHA, another antioxidant agent (data not shown). These effects of antioxidants on the JNK pathway were confirmed in IκBαM 3DO clones (data not shown), indicating that they extend to various cell types. We concluded that ROS accumulation is required for persistent induction of JNK by TNFα. Hence, in line with data recently reported by others (Sakon et al., 2003), ROS lie upstream of JNK in the apoptotic cascade induced by TNF-Rs.

Our findings predict that FHC inhibits JNK activation by TNFα. To test this hypothesis, we monitored TNFα-induced JNK signaling in cells expressing FHC or FHC-222 and in control cells. As shown previously, in *relA*$^{-/-}$ fibroblasts transduced with empty MIGR1 vectors, activation of JNK signaling by TNFα was rapid and remained sustained throughout stimulation (Figure 6B). Similar effects were observed in MIGR1-FHC-222-transduced cells. Remarkably, however, upon expression of FHC (MIGR1-FHC), JNK signaling returned to near-basal levels by 30 min (Figure 6B). FHC also slightly affected the acute phase of this signaling. Most importantly, knockdown of FHC by siRNA in wild-type NIH-3T3 fibroblasts resulted in markedly increased JNK induction by TNFα (Figure 6C). This exaggerated induction correlated with the dramatic sensitivity of these cells to cytokine-induced cytotoxicity (Figures 3E and 3F and Supplemental Figure S3). Indeed, in *fhc-198* siRNA-expressing fibroblasts, kinetics of TNFα-induced JNK activation were reminiscent of those seen in NF-κB-deficient cells (De Smaele et al., 2001). This suggests that FHC and NF-κB have similar effects on JNK activation in response to TNFα. We concluded that FHC halts TNFα-induced killing, at least in part, by suppressing JNK activation by ROS. These findings identify FHC as an indirect mechanism by which NF-κB controls the JNK cascade.

Discussion

We have identified FHC as a critical mediator of the NF-κB protective activity against TNFα-induced cytotoxicity. FHC is upregulated by TNFα through a mechanism that requires NF-κB (Figures 2A, 2C, and 2E), is essential to antagonize TNFα-induced killing (Figures 3E and 3F and Supplemental Figures S3, S4A, and S4B), and blocks PCD in NF-κB null cells (Figures 3A, 3B, 4A, 4B and Supplemental Figures S2A). FHC-mediated suppression of apoptosis involves inhibition of ROS accumulation (Figures 5A and 5B), which in turn prevents persistent activation of the JNK pathway (Figures 6A–6C). These findings identify FHC as a critical effector of NF-κB-mediated suppression of ROS and define an

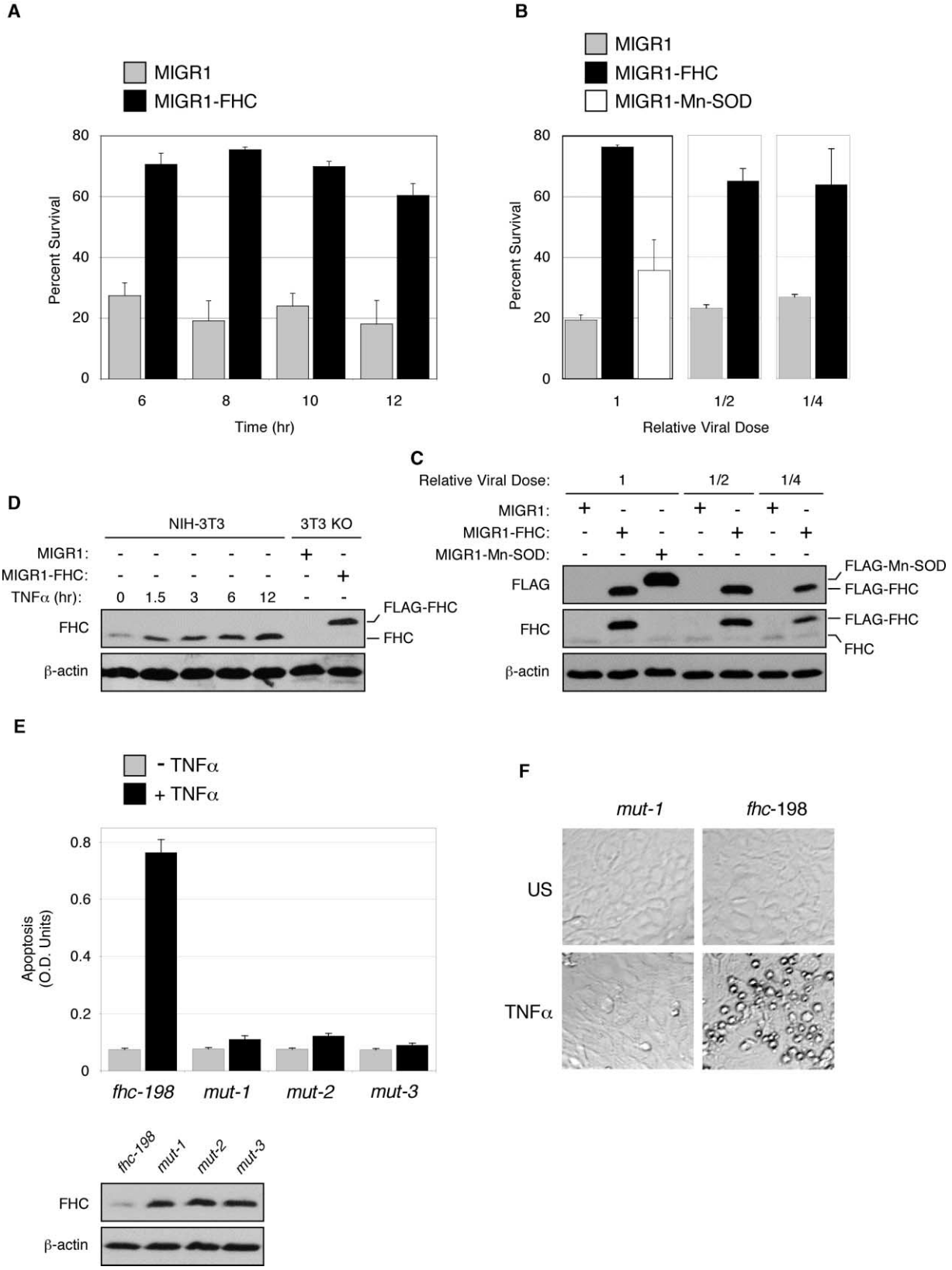

Figure 3. FHC Is a Physiologic Inhibitor of TNFα-Induced Killing

(A) FHC blocks TNFα-induced PCD in NF-κB null cells. Survival of MIGR1- and MIGR1-FHC-transduced *relA*$^{-/-}$ cells following treatment with TNFα (100 U/ml) plus CHX (0.1 μg/ml). Shown are the percentages of live (i.e., adherent) GFP^{+} cells (determined by manual counting and FCM) relative to the numbers observed in cultures treated with CHX alone. Values represent the mean ± standard deviation of three independent experiments.

essential mechanism by which NF-κB controls the JNK cascade and, ultimately, apoptosis.

FHC as a Mediator of the NF-κB Protective Function

In agreement with our findings, another study has recently implicated NF-κB in the inhibition of ROS induction by TNFα (Sakon et al., 2003). The antioxidant activity of NF-κB has been previously linked to upregulation of Mn-SOD (Bernard et al., 2001; Delhalle et al., 2002; Guo et al., 2003), which catalyzes dismutation of $O_2^{\cdot-}$ into H_2O_2 (Curtin et al., 2002). However, in various cells, Mn-SOD is induced by TNFα only poorly or at late times (Delhalle et al., 2002; Guo et al., 2003)—well after the onset of apoptosis. Moreover, in several NF-κB null systems, Mn-SOD expression affords only little or no protection against TNFα-induced killing (Brouard et al., 2002; Delhalle et al., 2002; Sakon et al., 2003; see also Figure 3B). Even in some wild-type systems, this factor seems to be a poor blocker of TNFα-induced PCD (Bernard et al., 2001). Yet, despite the modest antiapoptotic activity of overexpressed Mn-SOD, antioxidant treatment can effectively rescue NF-κB null cells from death (Delhalle et al., 2002; Sakon et al., 2003; Figures 1C–1E).

We found that Mn-SOD expression does not correlate with cytoresistance to TNFα. In 3DO cells, this enzyme was not upregulated by TNFα (or P/I), and its basal expression was independent of NF-κB (Figures 2A, 2B, and 2D). Furthermore, Mn-SOD exhibited weak protective activity in RelA null cells (Figure 3B; see also Sakon et al. [2003]). Consistently, Mn-SOD scored poorly in our microchip screen (Table 1). Thus, in 3DO cells and MEFs, this factor cannot be the sole effector of the antioxidant activity of NF-κB.

In contrast, FHC was induced rapidly by TNF-R ligation or P/I treatment, and this induction required NF-κB (Figures 2A–2D, Northern blots; see also Figures 2E and 2F, Western blots). In HeLa cells, selective activation of RelA was sufficient to upregulate FHC levels (Figure 2F). Indeed, the *fhc* promoter contains putative NF-κB binding DNA elements (Torti and Torti, 2002). Other antioxidant enzymes isolated from our screen do not appear relevant to the NF-κB-mediated control of apoptosis, as their expression was not modulated by TNFα, and their basal levels were independent of NF-κB (Figures 2A, 2B, and 2D). Likewise, *ho-1* was induced by TNFα but only at late times (Figures 2A and 2B)—well after activation of caspases (Figure 4A; De Smaele et al., 2001)—and its activation by P/I did not require NF-κB (Figure 2D).

FHC expression effectively blocked TNFα-induced ROS accumulation and PCD in RelA null fibroblasts (Figures 3A, 3B, 5A, and 5B and Supplemental Figure S2A; see also Figures 4A and 4B). Most importantly, silencing of FHC by siRNA in wild-type cells, which mimics the defective FHC expression seen in NF-κB null cells, enhanced TNFα-induced cytotoxicity (Figures 3E and 3F and Supplemental Figures S3, S4A, and S4B). In some systems, *fhc* downregulation is sufficient on its own to induce death (Yang et al., 2002; Cozzi et al., 2004). The biologic relevance of FHC is further underscored by the findings that, in fibroblasts, *fhc*- and *relA*-specific siRNAs have comparable effects on TNFα-induced PCD (Supplemental Figure S3) and that FHC levels capable of affording near-complete protection against this PCD can be found under physiological conditions (Figures 3A–3D and Supplemental Figure S2B). The early embryonic lethality of FHC knockout mice (Ferreira et al., 2000) further supports the importance of FHC for cell survival. Indeed, the relevance of FHC for the NF-κB-mediated control of PCD extends to human cell systems and cell types other than fibroblasts (Supplemental Figure S4B). Interestingly, downregulation of FHC expression is associated with a dramatic increase in intracellular ROS levels (Kakhlon et al., 2001; Cozzi et al., 2004) and exaggerated induction of JNK by TNFα (Figure 6C). Altogether, these findings identify FHC as a dominant mediator of the NF-κB-protective activity against ROS-mediated PCD and suggest that, at least in fibroblasts and HeLa cells, this factor is more relevant to this activity than previously described ROS scavengers.

ROS Inhibition in Cytoprotection against TNFα-Induced PCD

ROS play an obligatory role in the induction of apoptosis by TNF-Rs (Delhalle et al., 2002; Garg and Aggarwal, 2002; Matsuzawa et al., 2002; Sakon et al., 2003; also Figures 1C, 1D, and 1F and Supplemental Figure S1). Following receptor triggering, ROS accumulation precedes caspase activation and mitochondrial depolarization (Figures 1A, 4A, 4B, and 5A), and inhibition of this accumulation by various means blocks cytotoxicity (Figures 1C, 1D, and 1F and Supplemental Figure S1; see also Figures 3A, 3B, and 5A–5C; Delhalle et al., 2002; Garg and Aggarwal, 2002; Sakon et al., 2003). Proapoptotic activity of ROS is mediated in part by the JNK pathway (Garg and Aggarwal, 2002; Matsuzawa et al., 2002; Sakon et al., 2003). Indeed, inhibition of the JNK pathway represents a pivotal protective mechanism me-

(B) Unlike FHC, Mn-SOD exhibits only modest protective effects in NF-κB-deficient cells. Survival of *relA*$^{-/-}$ fibroblasts transduced with standard (1) or partial (1/2 and 1/4) doses of MIGR1, MIGR1-Mn-SOD, or MIGR1-FHC retroviruses and treated as in (A). Values represent the mean ± standard deviation of two independent experiments and are calculated as in (A).

(C) Cytoprotection correlates with FHC levels. Western blots showing FLAG-FHC and FLAG-Mn-SOD expression in the *relA*$^{-/-}$ cells used in (B). Antibodies are indicated on the left-hand side.

(D) Western blots showing FHC expression in TNFα-treated (1000 U/ml) NIH-3T3 fibroblasts and in MIGR1- and MIGR1-FHC-transduced *relA*$^{-/-}$ cells (3T3 KO). Equivalent amounts of extract (30 μg) were loaded in each lane. Endogenous and exogenous FHC are shown. FLAG-FHC levels are similar to those seen in (C), at relative viral dose 1 (data not shown).

(E) FHC is required to antagonize TNFα-induced killing in fibroblasts. ELISA assays showing apoptosis in NIH-3T3 lines stably expressing *fhc*-specific (*fhc-198*) or nonsilencing (*mut-1*, *-2*, and *-3*) siRNAs and treated for 9 hr with TNFα (250 U/ml) or left untreated (top). Values are expressed as arbitrary units and represent the mean ± standard deviation of three independent experiments. Western blots showing FHC and β-actin levels in the same NIH-3T3 lines (bottom).

(F) Phase contrast images of NIH-3T3 lines treated as in (E) for 16 hr. A 10× objective was used.

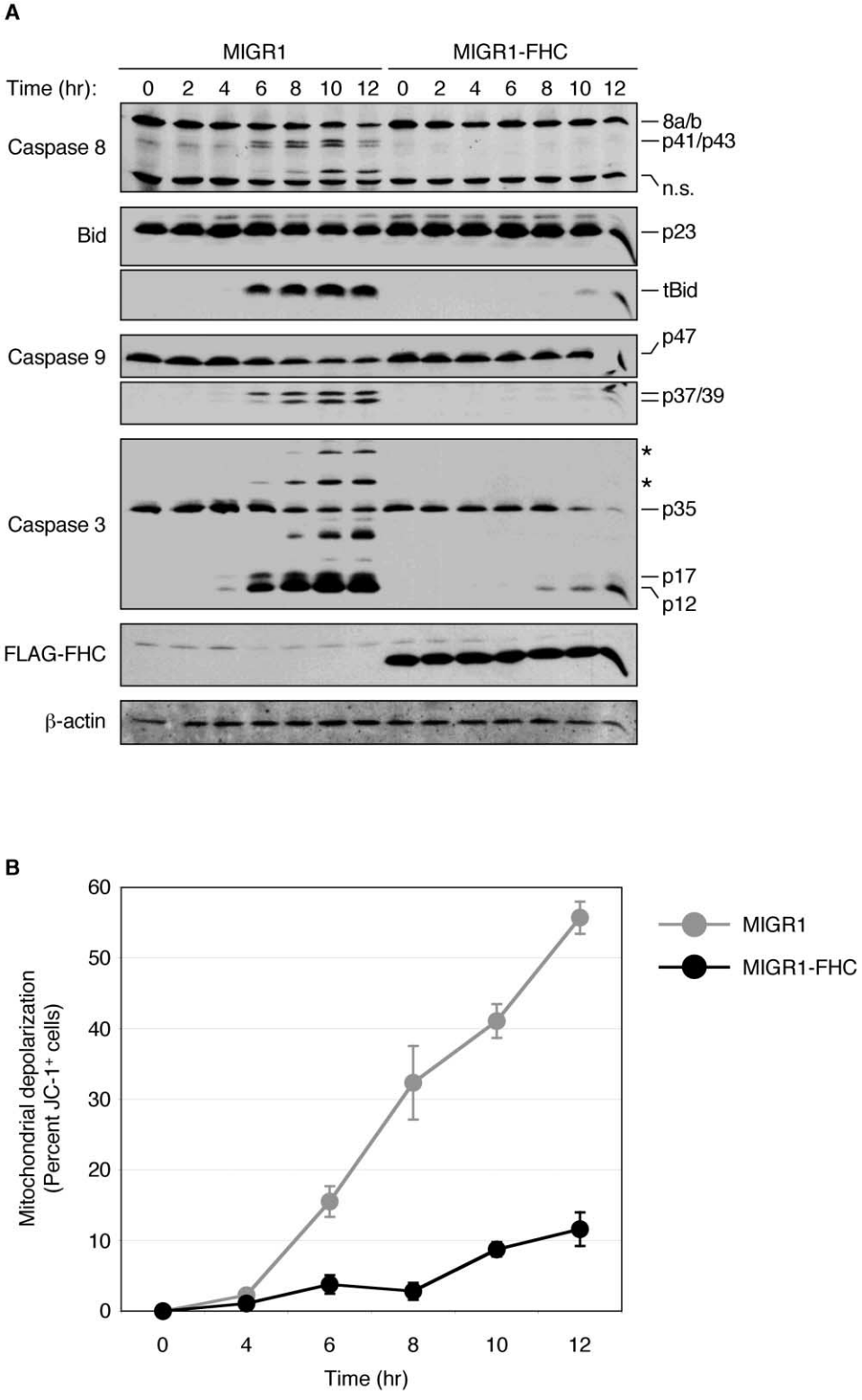

Figure 4. FHC Blocks Apoptosis Signaling in NF-κB Null Cells

(A) Western blots showing procaspase and Bid processing in MIGR1- and MIGR1-FHC-transduced *relA*$^{-/-}$ cells after treatment with TNFα (100 U/ml) plus CHX (0.1 μg/ml). Times, antibodies, cleavage products, and nonspecific (n.s.) bands are indicated. FLAG-FHC was detected with an anti-FLAG antibody.

(B) Mitochondrial depolarization in MIGR1- and MIGR1-FHC-transduced *relA*$^{-/-}$ fibroblasts treated as in (A). Values represent the percentages of JC-1^{+} cells relative to cultures treated with CHX alone and are the mean ± standard deviation of three independent experiments.

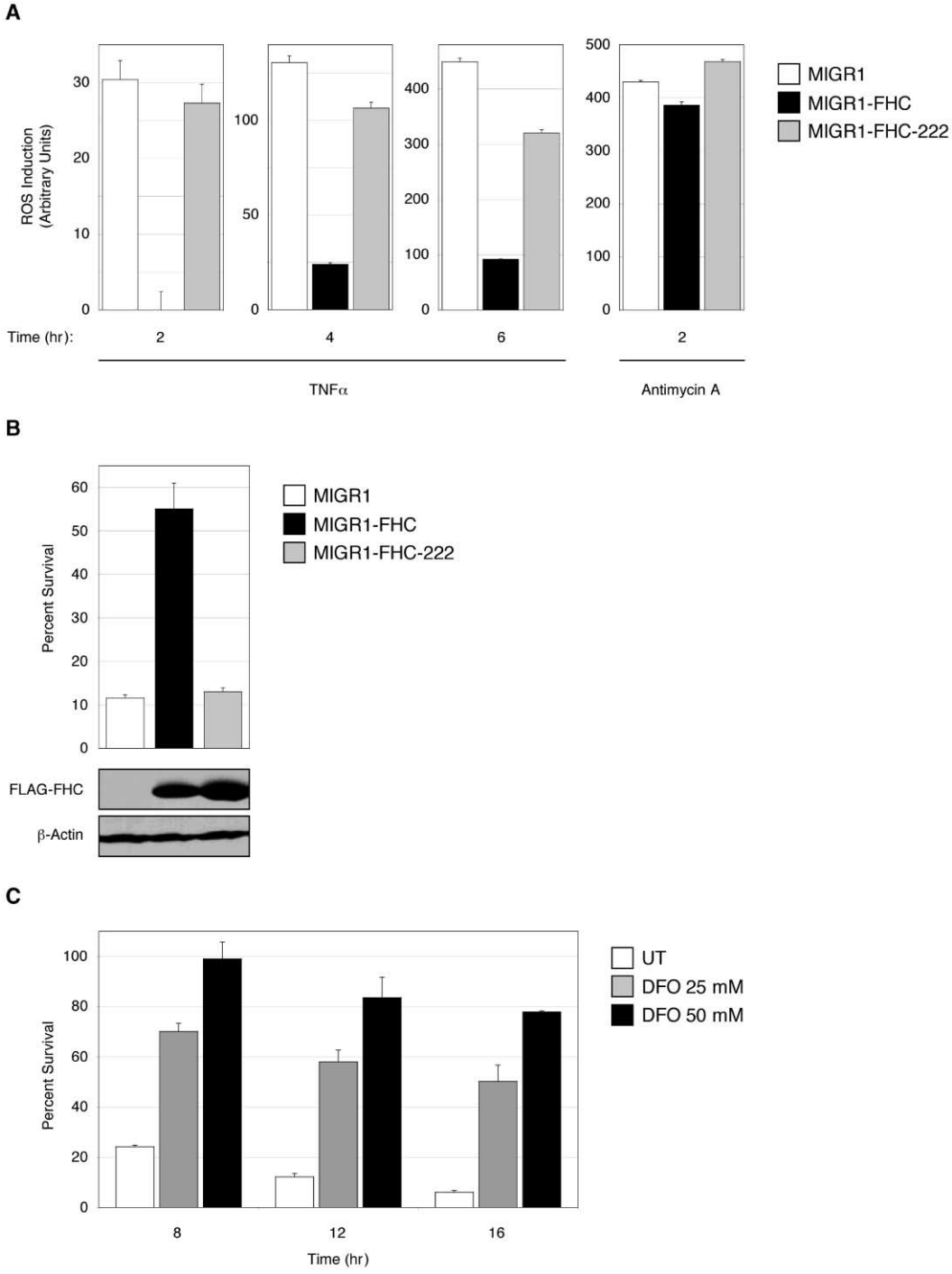

Figure 5. The FHC Inhibition of TNFα-Induced ROS Accumulation and Apoptosis Involves Iron Sequestration

(A) ROS inhibition by FHC requires iron binding activity. ROS induction by antimycin A (1 μg/ml) or TNFα (100 U/ml) plus CHX (0.1 μg/ml) in MIGR1-ΔGFP-, MIGR-ΔGFP-FHC-, and MIGR1-ΔGFP-FHC-222-transduced *relA*$^{-/-}$ cells. ROS measurements and value calculations were performed as in Figure 1A. Shown are the means (± standard deviations) of three independent measurements.

(B) Iron binding is essential for the FHC suppression of TNFα-induced PCD. Survival of MIGR1-, MIGR1-FHC-, and MIGR1-FHC-222-transduced *relA*$^{-/-}$ cells after a 9 hr treatment with TNFα (100 U/ml) plus CHX (0.1 μg/ml) (top). Percentages of live GFP^{+} cells were determined as in Figure 3A. Shown are the means ± standard deviations of three independent experiments. Western blots showing levels of β-actin, FLAG-FHC, and FLAG-FHC-222 (bottom and middle).

(C) Iron depletion protects NF-κB-deficient cells from TNFα-induced killing. PI nuclear staining showing survival of *relA*$^{-/-}$ cells treated with TNFα plus CHX as in (B) in the presence or absence of a 1 hr pretreatment with the indicated concentrations of DFO. Values were calculated as in Figure 1C and represent the means ± standard deviations of three independent experiments.

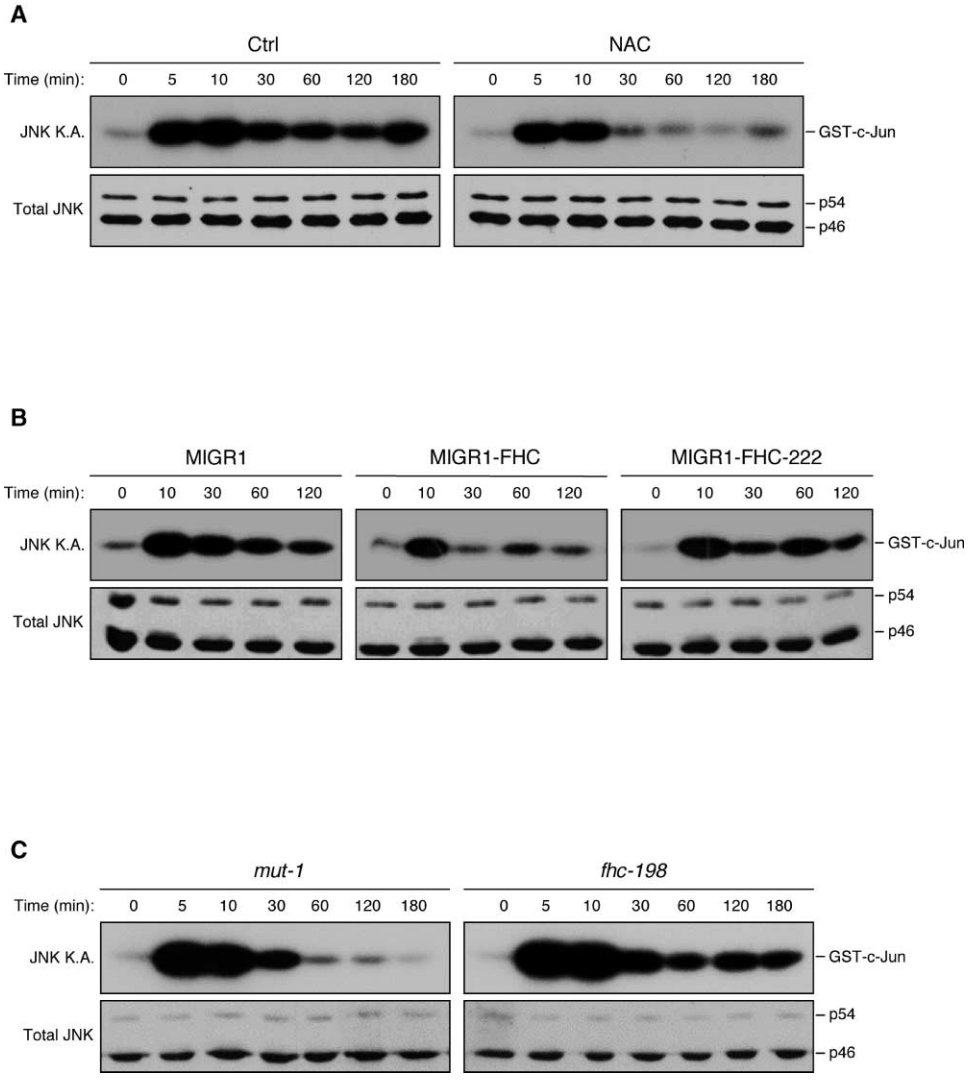

Figure 6. FHC Prevents Sustained JNK Induction by TNFα in NF-κB-Deficient Cells

(A) ROS are required for prolonged JNK activation by TNFα. Kinase assays (K.A.) showing JNK induction by TNFα (1000 U/ml) in *relA*$^{-/-}$ cells, in the presence or absence of a 20 min pretreatment with NAC (20 mM) (top). Western blots showing total JNK levels (bottom).

(B) FHC inhibits JNK induction by TNFα, and this activity involves iron sequestration. Kinase assays showing kinetics of JNK induction in MIGR1-, MIGR-FHC-, and MIGR1-FHC-222-transduced *relA*$^{-/-}$ cells treated with TNFα as in (A) (top). Western blots showing total JNK levels (bottom).

(C) FHC is required for downmodulation of TNFα-induced JNK signaling. Kinase assays showing JNK activation in NIH-3T3 lines expressing *fhc*-specific or nonsilencing (*mut-1*) siRNAs and treated with TNFα as in (A) (top). Western blots showing total JNK levels (bottom). FHC expression is shown in Figure 3E.

diated by NF-κB (De Smaele et al., 2001; Javelaud and Besancon, 2001; Tang et al., 2001), and knockdown of the JNK kinase MKK7/JNKK2 rescues RelA null cells from TNFα-induced killing (Deng et al., 2003). Notably, the relevance of the crosstalk between NF-κB and JNK to cell survival has been documented in animal models by using JNK knockout systems (Maeda et al., 2003). Our data support a model whereby NF-κB activation upregulates expression of FHC, which sequesters free iron, and so blunts ROS production, sustained JNK signaling, and, ultimately, apoptosis triggered by TNFα.

The Suppression of JNK Signaling by NF-κB

Our findings identify FHC as an additional link between the NF-κB and JNK pathways. Previously, we have shown that suppression of JNK signaling by NF-κB involves induction of Gadd45β (De Smaele et al., 2001). However, this induction cannot explain the effects of NF-κB on redox metabolism (Sakon et al., 2003; Figure 1A). Thus, we propose that NF-κB halts the JNK cascade via at least two distinct mechanisms: directly, through Gadd45β-mediated blockade of MKK7 (Papa et al., 2004), and indirectly, through FHC, which blunts ROS production. To ensure effective inhibition of JNK signaling, Gadd45β and FHC likely act in concert. Indeed, kinetics of induction suggest that transient activation of Gadd45β may provide acute protection against TNFα-induced toxicity and that sustained FHC upregulation serves to secure long-term survival. FHC may also cooperate with Mn-SOD. It is conceivable that, while upregu-

lation of Mn-SOD promotes $O_2^{\cdot-}$ dismutation into H_2O_2 (Curtin et al., 2002), FHC-mediated iron depletion allows disposal of H_2O_2 by catalases and peroxidases, thereby preventing formation of highly reactive ·OH radicals (Torti and Torti, 2002). Indeed, residual availability of iron, resulting from FHC deficiency, may explain why Mn-SOD alone is unable to effectively suppress TNFα-induced PCD in NF-κB null cells (Figure 3B; Brouard et al., 2002; Delhalle et al., 2002; Sakon et al., 2003). While not sufficient, however, Mn-SOD might still be needed for the NF-κB antiapoptotic function in some biological contexts.

Relevance to Chronic Inflammation and Cancer

Notably, the protective effects of FHC likely extend beyond the cellular level and may, in fact, mediate a systemic defense mechanism activated by NF-κB. FHC is a component of the organismal acute phase response to stress, injury, and infection (Torti and Torti, 2002; Weiss, 2002). Proinflammatory cytokines such as TNFα profoundly impact iron metabolism, and induction of FHC synthesis in the liver appears to be a major cause of hypoferraemia and anemia during chronic inflammation (Torti and Torti, 2002; Weiss, 2002). Thus, generalized restriction of metal availability may enable NF-κB to contain cytokine-induced injury at distant sites, such as, for instance, at sites of inflammation, where there are high levels of TNFα and oxygen radicals. Consistent with this notion, systemic iron depletion by DFO markedly protects mice from TNF-R-mediated tissue damage and lethality (Vulcano et al., 2000).

FHC also plays an important role in cancer (Torti and Torti, 2002). During malignant transformation, FHC expression is repressed by oncogenes such as c-Myc and adenovirus E1A (Arosio and Levi, 2002; Torti and Torti, 2002). This repression is associated with an increase in intracellular free iron and ROS levels (Benhar et al., 2002; Cozzi et al., 2004; Kakhlon et al., 2001; Tanaka et al., 2002; Torti and Torti, 2002), which promote apoptosis, both under basal conditions and upon treatment with chemotherapeutic drugs (Benhar et al., 2002). In the early stages of cancer, this elevation of ROS (and JNK activity) appears to be critical for proliferation and maintenance of a transformed phenotype (Benhar et al., 2002). With tumor progression, however, growth becomes independent of ROS (Benhar et al., 2002), which allows cancer cells to upregulate FHC, thereby promoting tumor resistance to anticancer agents (Torti and Torti, 2002). Indeed, the protective activity of FHC extends to oxidative and genotoxic stress (Arosio and Levi, 2002; Torti and Torti, 2002), and high FHC levels have been associated with an aggressive malignant phenotype (Torti and Torti, 2002). Thus, FHC may contribute to NF-κB-dependent cancer chemoresistance and thereby represent a potential therapeutic target.

Experimental Procedures

Library Construction and Selection

The pLTP-GFP vector used for library construction was generated by inserting the ~0.75 kb SmaI-BsrG1 fragment of pEGFP-N1 (Clontech, Palo Alto, CA) into the EcoRV and NotI sites of pLTP (Vito et al., 1996) along with the following oligonucleotide linker: 5′-*GTA CAAG*GCCTCGAGGGCCTCATGAATCAGTCAGCGGCCGC**TGACT AACG**T**AG***TG*-3′ (sense strand: stop codons are in bold; partial BsrG1 and destroyed NotI sites are italicized; internal SfiI, XhoI, BspHI, and NotI sites are underlined). For cDNA synthesis, poly-A mRNA was isolated from NIH-3T3 cells treated with TNFα (1000 U/ml) for 2.5 or 5.5 hr, and reverse transcriptase (RT) reaction was set up using pooled mRNA samples, an oligo(dT) primer (containing a NotI site), and the Superscript II kit (Invitrogen, Carlsbad, CA), according to manufacturer's instructions. Upon size fractionation, the cDNA was ligated to SfiI adaptors (sense, 5′-GAAGCCCTCG-3′; anti-sense, 5′-GGGCTTC-3′), digested with NotI, and cloned directionally into the NotI and SfiI sites of pLTP-GFP. This library yielded 1.8×10^6 independent clones, had an average insert size of ~1.7 kb, and expressed polypeptides fused to enhanced green fluorescent protein (eGFP).

Library selection was carried out essentially as described previously (De Smaele et al., 2001). Briefly, 4×10^6 independent library clones were transfected into *relA*$^{-/-}$ 3T3 cells by using the DEAE method. Twenty-four hours later, cells were subjected to a 21 hr treatment with TNFα (150 U/ml) plus cycloheximide (CHX; 0.1 μg/ml). Detached cells were then washed away, and adherent (live) cells were trypsinized, purified with Lympholyte Ficoll (Accurate Chemical and Scientific Corp., Westbury, NY), and resuspended in lysis solution (0.6% SDS and 10 mM EDTA) for extraction of episomal DNA. The library was finally electroporated into ElectroMax DH10B *E. coli* (Invitrogen, Carlsbad, CA), amplified, and used for another cycle of selection in *relA*$^{-/-}$ cells.

cRNA Probe Preparation and Microarray Analyses

To generate biotinylated cRNA probes, original and selected libraries were treated with RNase and Proteinase K in 0.5% SDS, digested with BsrGI, and subjected to in vitro transcription (IVT) using the SP6 RNA polymerase MEGAscript kit (Ambion Inc., Austin, TX) and biotinylated UTP and CTP (Enzo Diagnostic, Farmingdale, NY). Probe hybridizations to Mu6500 oligonucleotide microarrays (representing ~6,500 murine genes; Affymetrix, Santa Clara, CA) were performed according to standard procedures at Research Genetics (Huntsville, AL). Comparative analyses of signal intensities (SI) were carried out using the Affymetrix Microarray Suite 5.0 (MAS v5.0) with default analytic parameters, and genes were ranked according to their SLR value (as defined in the Affymetrix Statistical Algorithms Description Document). This value represents the change in SI for a cDNA between original (baseline) and selected libraries and is expressed as $\log_2$ ratio.

ROS Measurements

Dichlorodihydrofluorescein diacetate (H_2DCFDA) was from Molecular Probes (Eugene, OR). Intracellular ROS levels were measured as described elsewhere (Chandel et al., 2001). Briefly, 30 min prior to adding TNFα or antimycin A, cultures were treated with 25 μM H_2DCFDA in phenol red-free and serum-free DMEM. At the times indicated, cells were lysed in luciferase buffer (Chandel et al., 2001), and H_2DCFDA oxidation into 2′,7′ dichlorofluorescein (DCF) was measured by spectrofluorometric analysis at 485 nm (excitation) and 528 nm (emission) using a FLx 800 reader (Bio-Tek Instruments, Inc., Winooski, VT). Further information regarding DFO and H_2DCFDA and their applications can be found in the Supplemental Data.

Additional Methods

Information on additional methods, plasmids, cells, and reagents can be found in the Supplemental Data.

Acknowledgments

We thank N. Chandel, L. D'Adamio, M. Peter, G. Getz, J. Crispino, J. Knabb, and P. Ashton-Rickardt for helpful discussions and critical comments. We also thank P. Schumacker for reagents, C. Gelinas for the HtTA cell lines, A. Hayes for editorial help, and M. Jurkiewicz for help with Western blots. Supported in part by the Damon Runyon Scholar Award and NIH grant RO1CA84040. C.G.P. is supported in part by NIH Cardiovascular Pathophysiology training grant HL07237. S.V.T. and F.M.T. are supported by NIH grant DK42412.

Received: March 30, 2004
Revised: September 7, 2004
Accepted: October 1, 2004
Published: November 11, 2004

References

Arosio, R., and Levi, S. (2002). Ferritin, iron homeostasis, and oxidative damage. Free Radic. Biol. Med. *33*, 457–463.

Benhar, M., Engelberg, D., and Levitzki, A. (2002). ROS, stress-activated kinases and stress signaling in cancer. EMBO Rep. *3*, 420–425.

Bernard, D., Quatannens, B., Begue, A., Vandenbunder, B., and Abbadie, C. (2001). Antiproliferative and antiapoptotic effects of cRel may occur within the same cells via the upregulation of manganese superoxide dismutase. Cancer Res. *61*, 2656–2664.

Brouard, S., Otterbein, L.E., Anrather, J., Tobiasch, E., Bach, F.H., Choi, A.M.K., and Soares, M.P. (2000). Carbon monoxide generated by heme oxygenase 1 suppresses endothelial cell apoptosis. J. Exp. Med. *192*, 1015–1025.

Brouard, S., Berberat, P.O., Tobiasch, E., Seldon, M.P., Bach, F.H., and Soares, M.P. (2002). Heme oxygenase-1-derived carbon monoxide requires the activation of transcription factor NF-κB to protect endothelial cells from tumor necrosis factor-α-mediated apoptosis. J. Biol. Chem. *277*, 17950–17961.

Chandel, N., Schumacker, P.T., and Arch, R.H. (2001). Reactive oxygen species are downstream products of TRAF-mediated signal transduction. J. Biol. Chem. *276*, 42728–42736.

Chang, L., and Karin, M. (2001). Mammalian MAP kinase signaling cascades. Nature *410*, 37–40.

Cozzi, A., Levi, S., Corsi, B., Santambrogio, P., Campanella, A., Gerardi, G., and Arosio, P. (2003). Role of iron and ferritin in TNFα-induced apoptosis in HeLa cells. FEBS Lett. *537*, 187–192.

Cozzi, A., Corsi, B., Levi, S., Santambrogio, P., Biasiotto, G., and Arosio, P. (2004). Analysis of the biologic functions of H- and L-ferritins in HeLa cells by transfection with siRNAs and cDNA: evidence for a proliferative role for L-ferritin. Blood *103*, 2377–2383.

Curtin, J.F., Donovan, M., and Cotter, T.G. (2002). Regulation and measurement of oxidative stress in apoptosis. J. Immunol. Methods *265*, 49–72.

Danial, N.N., and Korsmeyer, S.J. (2004). Cell death: critical control points. Cell *116*, 205–219.

Davis, R.J. (2000). Signal transduction by the JNK group of MAP kinases. Cell *103*, 239–252.

Delhalle, S., Deregowski, V., Benoit, V., Merville, M.P., and Bours, V. (2002). NF-κB-dependent MnSOD expression protects adenocarcinoma cells from TNFα-induced apoptosis. Oncogene *21*, 3917–3924.

Deng, Y., Ren, X., Yang, L., Lin, Y., and Wu, X. (2003). A JNK-dependent pathway is required for TNFα-induced apoptosis. Cell *115*, 61–70.

De Smaele, E., Zazzeroni, F., Papa, S., Nguyen, D.U., Jin, R., Jones, J., Cong, R., and Franzoso, G. (2001). Induction of *gadd45β* by NF-κB downregulates proapoptotic JNK signaling. Nature *414*, 308–313.

Ferreira, C., Bucchini, D., Martin, M.E., Levi, S., Arosio, P., Grandchamp, B., and Beaumont, C. (2000). Early embryonic lethality of H ferritin gene deletion in mice. J. Biol. Chem. *275*, 3021–3024.

Fleury, C., Mignotte, B., and Vayssiere, J.L. (2002). Mitochondrial reactive oxygen species in cell death signaling. Biochimie *84*, 131–141.

Garg, A.K., and Aggarwal, B.B. (2002). Reactive oxygen intermediates in TNF signaling. Mol. Immunol. *39*, 509–517.

Gerondakis, S., and Strasser, A. (2003). The role of Rel/NF-κB transcription factors in B lymphocyte survival. Semin. Immunol. *15*, 159–166.

Ghosh, S., May, M.J., and Kopp, E.B. (1998). NF-κB and rel proteins: evolutionarily conserved mediators of immune responses. Annu. Rev. Immunol. *16*, 225–260.

Guo, Z., Boekhoudt, G.H., and Boss, J.M. (2003). Role of the intronic enhancer in tumor necrosis factor-mediated induction of manganous superoxide dismutase. J. Biol. Chem. *278*, 23570–23578.

Javelaud, D., and Besancon, F. (2001). NF-κB activation results in rapid inactivation of JNK in TNFα-treated Ewing sarcoma cells: a mechanism for the antiapoptotic effect of NF-κB. Oncogene *20*, 4365–4372.

Kakhlon, O., Gruenbaum, Y., and Cabantchik, Z.I. (2001). Repression of ferritin expression increases the labile iron pool, oxidative stress, and short term growth of human erythroleukemia cells. Blood *97*, 2863–2871.

Kucharczak, J., Simmons, M.J., Fan, Y., and Gelinas, C. (2003). To be, or not to be: NF-κB is the answer—role of Rel/NF-κB in the regulation of apoptosis. Oncogene *22*, 8961–8982.

Leist, M., and Jaattela, M. (2001). Four deaths and a funeral: from caspases to alternative mechanisms. Nat. Rev. Mol. Cell Biol. *2*, 1–10.

Maeda, S., Chang, L., Li, Z.W., Luo, J.L., Leffert, H., and Karin, M. (2003). IKKβ is required for prevention of apoptosis mediated by cell-bound but not by circulating TNFα. Immunity *19*, 725–737.

Matsuzawa, A., Nishitoh, H., Tobiume, K., Takeda, K., and Ichijo, H. (2002). Physiological roles of ASK1-mediated signal transduction in oxidative stress- and endoplasmic reticulum stress-induced apoptosis: advanced findings from ASK1 knockout mice. Antioxid. Redox Signal. *4*, 415–425.

Orlowski, R.Z., and Baldwin, A.S. (2002). NF-κB as a therapeutic target in cancer. Trends Mol. Med. *8*, 385–389.

Papa, S., Zazzeroni, F., Bubici, C., Jayawardena, S., Alvarez, K., Matsuda, S., Nguyen, D.U., Pham, C.G., Nelsbach, A.H., Melis, T., et al. (2004). Gadd45β mediates the NF-κB suppression of JNK signalling by targeting MKK7/JNKK2. Nat. Cell Biol. *6*, 146–153.

Sakon, S., Xue, X., Takekawa, M., Sasazuki, T., Okazaki, T., Kojima, Y., Piao, J.H., Yagita, H., Okumura, K., Doi, T., and Nakano, H. (2003). NF-κB inhibits TNF-induced accumulation of ROS that mediate prolonged MAPK activation and necrotic cell death. EMBO J. *22*, 3898–3909.

Smirnov, I.M., Bailey, K., Flowers, C.H., Garrigues, N.W., and Wesselius, L.J. (1999). Effects of TNF-α and IL-1β on iron metabolism by A549 cells and influence of cytotoxicity. Am. J. Physiol. *277*, L257–L263.

Tanaka, H., Matsumura, I., Ezoe, S., Satoh, Y., Sakamaki, T., Albanese, C., Machii, T., Pestell, R.G., and Kanakura, Y. (2002). E2F1 and c-MYC potentiate apoptosis through inhibition of NF-κB activity that facilitates MnSOD-mediated ROS elimination. Mol. Cell *9*, 1017–1029.

Tang, G., Minemoto, Y., Dibling, B., Purcell, N.H., Li, Z., Karin, M., and Lin, A. (2001). Inhibition of JNK activation through NF-κB target genes. Nature *414*, 313–317.

Torti, F.M., and Torti, S.V. (2002). Regulation of ferritin genes and proteins. Blood *99*, 3505–3516.

Vito, P., Lacana, E., and D'Adamio, L. (1996). Interfering with apoptosis: Ca2+-binding protein ALG-2 and Alzheimer's disease gene ALG-3. Science *271*, 521–525.

Vulcano, M., Meiss, R.P., and Isturiz, M.A. (2000). Deferoxamine reduces tissue injury and lethality in LPS-treated mice. Int. J. Immunopharmacol. *22*, 635–644.

Weiss, G. (2002). Pathogenesis and treatment of anaemia of chronic disease. Blood Rev. *16*, 87–96.

Yang, D.C., Jiang, X., Elliott, R.L., and Head, J.F. (2002). Antisense ferritin oligonucleotides inhibit growth and induce apoptosis in human breast carcinoma cells. Anticancer Res. *22*, 1513–1524.

Zong, W.X., Edelstein, L.C., Chen, C., Bash, J., and Gelinas, C. (1999). The prosurvival Bcl-2 homology Bfl-1/A1 is a direct transcriptional target of NF-κB that blocks TNFα-induced apoptosis. Genes Dev. *13*, 382–387.